

Research Article

Multithreshold Image Segmentation and Computer Simulation Based on Interactive Processing System

Liang Dong , Ding Gangyi , Yan Dapeng , and Huang Kexiang 

School of Computer Science, Beijing Institute of Technology, Beijing 100081, China

Correspondence should be addressed to Liang Dong; dong_630@bit.edu.cn

Received 1 May 2022; Revised 3 June 2022; Accepted 23 June 2022; Published 8 July 2022

Academic Editor: Imran Shafique Ansari

Copyright © 2022 Liang Dong et al. This is an open access article distributed under the Creative Commons Attribution License, which permits unrestricted use, distribution, and reproduction in any medium, provided the original work is properly cited.

With the increasing application of interactive processing systems at all levels, in order to better and efficiently spread the application range of interactive processing systems, this study has researched and developed an application system for interactive online processing of DVB-SMODIS data. In addition, correct and improved algorithms are proposed for most of the problems in DVB-SMODIS data. In order to better improve the overall search ability of the BBO algorithm in multithreshold image segmentation, this study discusses a new BBO algorithm. Image segmentation is an important processing part of digital image processing systems and computer vision systems. The use of computer simulation programming technology can simulate and replace the process of objects to produce simulation maps. According to the original object calculated by the computer system, it can be reconstructed and reproduced by referring to the mathematical formula of light waves and using traditional simulation technology experiments. Therefore, this article uses interactive processing technology to study the multithreshold graph segmentation and computer simulation technology.

1. Introduction

In the existing network environment, the interactive processing system technology has been further improved. The threshold value from data visualization products and the distributed processing of graphic data have become a new direction for the expansion of interactive processing system [1]. This technology not only saves the use space but also shortens the occupied network resources and reduces the computing resources. In addition, professional remote detection technology is added, which provides a convenient and efficient interactive method for nonprofessional personnel [2]. On this basis, it is more conducive to the in-depth use of interactive processing system at all levels. Because people get and transfer information through language, text, and image, vision is the first. Therefore, multithreshold image segmentation is more accurate than all other methods, which makes it the most important and frequently used way of information transmission [3]. With the widespread use and popularity of digital computer, artificial intelligence system, mobile phone, and image digital camera, the way to

get images is faster. The meaning of multithreshold image is that its image is composed of digital value pixels, and its basic elements are what we call pixels [4]. People transform the pixels in the multithreshold image in a specific way, so as to separate or deepen the overall image, and then through the next image features to extract the relevant information that we need and need to find [5]. Computer simulation is a subject technology that uses a computer system and its associated sensing equipment to imitate people's visual system [6]. According to the previous research and in-depth understanding, the most important way for people to feel and obtain information from the outside world is from vision, because the amount of information available in the human brain is based on perception, the amount of information available is large, and the use level is very high, so vision has become a very important way for people to access external information. People find out what they care about through vision, find satisfactory goals in time, make corresponding and correct judgments quickly, and finally complete their cognition of all things around [7]. To sum up, in recent years, some researchers have put forward their own

new views. According to the proposed point of view, the current multithreshold image segmentation algorithm is modified and improved, or combined with other different kinds of algorithms [8]. Compared with the traditional algorithm, the multithreshold image segmentation algorithm has greatly improved the computing time and complexity of modern image. The main research of this study is based on the existing, intelligent optimization algorithm of multithreshold image segmentation technology, synchronous image processing technology, to meet the requirements of the actual system application of image timely and effective processing [9]. Computer simulation technology uses low wave interference to capture the light source of the object. When the object is connected to the connected light source, the reference light wave is added to destroy the light wave object. This is the development era of computer simulation [10].

2. Related Work

The progress and growth of interactive processing system are explained in detail in literature [11]. The introduction of spatial database and spatial database engine makes the publication and operation of interactive processing system greatly improved. Meanwhile, the distribution of interactive processing system is mainly composed of special geographic information publishing objects. This study introduces the structure of remote sensing image data publishing system, which allows users to search for the target image by browser and then search the data according to the relevant requirements of users. Then, the search data is started through its engine, and the results of the search are returned to the users, so that users can view the relevant contents and make choices [12]. The literature is based on the modified and improved BBO algorithm, and then the corresponding simulation experiments are carried out. In order to facilitate the comparison of experimental results, the experimental results are compared with other kinds of multithreshold image segmentation methods. From the experimental results, the proposed algorithm can be shown to have a better segmentation effect compared with other algorithms. This study explains the wide application of computer simulation technology. According to the characteristics of interference image, we can judge the properties of the recorded objects, the effect of the recorded images, and the processing methods adopted [13]. The ability of studying phenomenon processing has been greatly improved. In the research, we find better improvement methods and better use of simulation technology are the starting points of the research. The literature shows the image segmentation method we used most. It only uses one-dimensional gray in the threshold selection, and the important information such as image edge obtained by it has not been referenced. So when the image is more complex, the obtained graph is more ambiguous. Therefore, in order to improve the substantive problems such as image blur, based on the two-dimensional cross entropy multithreshold image segmentation, this paper proposes to use the tilt method instead of the direct segmentation method to improve the fuzziness of

multithreshold image segmentation technology in calculation [14]. According to its own unique advantages and characteristics, it is applied to the multithreshold selection of image segmentation, so that it can be used to achieve the best segmentation threshold in a short time. The original multithreshold segmentation method is proposed in the literature. It is based on the search of the best segmentation threshold within the existing evaluation function. The search range is wide, which makes the calculation very difficult. Today, the intelligent optimization algorithm is the most important method to solve. In practice, although it may not be able to obtain the best results, it can obtain satisfactory solutions in a short time.

3. Design and Implementation of Interactive Processing System

3.1. Database Technology of Interactive Processing System.

In today's society, interactive processing system continues to develop. In the face of such a huge amount of remote sensing data, how to efficiently integrate remote sensing data has always been the most important thing in the application of remote sensing data. In order to improve the efficiency and function of interactive processing system database, many research technologies have been developed in the world, including the following aspects:

3.1.1. Preprocessing Technology of Interactive Processing System.

Because of the huge amount of data in the interactive processing system, it is not necessary for users to operate the whole image when they view and browse on the client. However, in today's network environment, the interactive processing system is limited by the bandwidth, and many data in the transmission process will affect the time of the system to a large extent, so the more rapid and reliable efficient searching and viewing of remote sensing image data are keys to improve the overall system efficiency. In order to improve the efficiency of remote sensing information search, it is necessary to preprocess the interactive processing system.

Remote Sensing Image Segmentation. The meaning of remote sensing image segmentation is that it is carried out according to a certain form, it is divided into data blocks with the same size, and then these remote sensing images are divided into blocks according to the corresponding arrangement, which is the basis of the establishment of the overall database. If the size of the data block segmented in this study is too small, but there are many actual data blocks, then it will increase the working time of the system when reading the data, but if the size of the data block is too large, then it will cause certain loss, so we must divide the remote sensing image reasonably.

Image Indexing Technology. In the process of publishing massive remote sensing data, the key to quickly and accurately meet the needs of users and search the required data in different ranges and spatial resolutions is image indexing technology. It is the related data that can be found by

conforming to the metadata of remote sensing image and the retrieval requirements of users. However, through the retrieval of data in a specific geographical area, the spatial relationship between the data and the image is used to realize the data search within the search scope, which belongs to the spatial data query. Nowadays, the commonly used spatial location index is usually divided from top to bottom and level by level. The most frequently used is the quadtree index.

Image Splicing and Caching Technology. When users view image data in different areas, they also need to acquire other images around them for splicing processing, so that the server will be sent with relevant requirements again. If every request needs to send requirements to the server according to the user's retrieval range and resolution, the data block acquired again will not only increase the reading and writing of the database but also increase the load of network transmission, which leads to the delay of the time users get data. However, if caching technology is used in the system, then its efficiency will be greatly improved.

Image Compression Technology. In today's network environment, the amount of image data is very large, which will lead to the efficiency of data transmission. In order to improve the transmission efficiency, we should study how to compress it. The most commonly used compression methods are lossy compression algorithm, MrSID, JPEG, etc. But in practical application, the above-mentioned compression algorithm will still appear the image unclear, which seriously affects the image effect of users. Therefore, this study decides to use the method of discrete wavelet transform to compress the data, so that the image can be preserved well and is also widely used nowadays.

3.1.2. Remote Sensing Data Storage Technology. The interactive processing system in the early days was only stored in the hard disk in the form of files, which was not conducive to the management, storage, and distribution of image data, and the security performance was very poor. However, with the development and technology of the relational database, a better remote sensing data storage method was developed. The method is to establish a separate remote sensing image database, which can improve its own efficiency and store the remote sensing information data separated from it in a database. It can only connect metadata with remote sensing image through unique signal sources. In this way, the retrieval efficiency of remote sensing data can be greatly improved. However, there are still many problems to be solved in the present remote sensing image storage mode.

3.2. Architecture Design of Interactive Processing System. Based on the existing widely used remote sensing image online processing system architecture and core technology understanding and analysis, this study uses the B/S system architecture, uses IIS as the web server, and uses ASP technology to study the overall system. The system uses interactive network interface, client event processing, and remote sensing image background processing, and is written

in C# language and IDL language. ArcSDE is used to build the system spatial database, and the storage management of remote sensing data uses Microsoft SQL Server and Google Maps as the designated tool for the spatial retrieval area. The construction system of the system is shown in Figure 1.

According to the specific use of the system, the function of the system is designed, as shown in Figure 2.

3.3. Database Design of Interactive Processing System. The key of the whole system is to establish a complete remote sensing image database. According to the existing whole system, the spatial database engine and relational database are used to complete the data storage management. Therefore, according to the user's requirements, this study mainly extracts the attribute data in Table 1.

Data level refers to the classification of data according to certain rules. The classification standards are listed in Table 2.

Image data classification refers to the classification according to the application scope of data. Its main purpose is to facilitate users to narrow the area of data search in the process of search. The main corresponding relations are listed in Table 3.

4. Multithreshold Image Segmentation and Computer Simulation

4.1. Multithreshold Image Segmentation. In today's society, GA and PSO algorithms have been used in multithreshold image segmentation. Moreover, the experimental results show that the solution quality and convergence speed are very good. In order to verify whether the improved BBO algorithm is really effective, we compare it with the algorithm mentioned above. In the process of this experiment, this study takes the cross-entropy function as the objective function and sets it as the evaluation function. In order to finally verify the effectiveness of the improved BBO algorithm mentioned in this study, this study prepares the following two groups of experiments to compare the image effect.

According to the above experiments, we can get from the results that, when one-dimensional multithreshold segmentation is used for sailboat multithreshold segmentation, we can clearly see that some information of the image has been lost. For example, the shadow of trees on shore is different from the shadow of ships in the water. The results of one-dimensional multithreshold segmentation are relatively stiff, but the results of two-dimensional segmentation are relatively natural. In addition, it can also be obtained from the experimental segmentation results of 3 and 4 thresholds, and some of the results of one-dimensional segmentation are missing; for example, the clouds in the image basically disappear, and the edges of trees and other important target areas are blurred. In the one-dimensional multithreshold segmentation of leaves, the more important part of the image still cannot be segmented. For example, from the experimental results of 2-threshold and 3-threshold segmentation, we can find that the diseased part of leaves is not completely

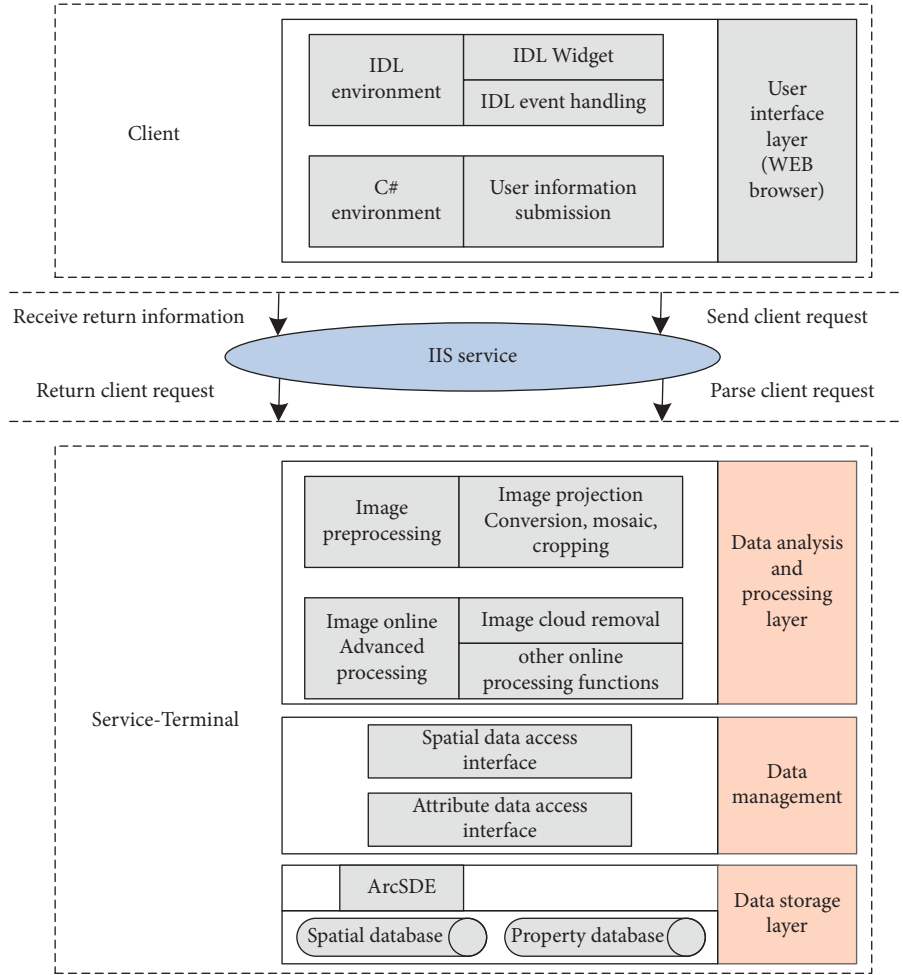


FIGURE 1: System structure diagram.

segmented. From the experimental results, we can see that each feature in the image is relatively stiff, and the edges of the image are not all displayed. In addition, it can be seen from the 4-threshold segmentation result image that the results of one-dimensional segmentation are not all displayed, for example, the leaf, main stem vein, and other important areas in the image.

According to the experiment set in this study, the following segmentation results are obtained under different thresholds. In the existing network environment of intelligent optimization algorithm, the multithreshold selection problem has developed a lot of fast and useful algorithms, such as genetic algorithm and particle swarm optimization algorithm. The experimental results are very good in the calculation quality and convergence rate. Therefore, in order to verify the effectiveness of the improved GSA algorithm mentioned in this study, based on the multithreshold image segmentation of the maximum entropy method, this study compares it with GSA, PSO, and GA. In this experiment, the entropy function is used as the standard function and evaluation function.

In the graph expression in Figure 3, it can be clearly observed that with the increase of the number of threshold bits, the algorithm time is also increasing.

4.2. Computer Simulation. After a series of processes, the light waves emitted by objects contain the relevant information of objects, and this information exists in any plane transmitted by the light waves propagating between each other. This is because the light of the information of the object is received. Therefore, when recording the wavefront of the light wave carrying the object information on a specific plane, we can use the appropriate time and place to reproduce the light wave, and then we can reproduce the original image of the object emitting light. When the hologram uses the principle of light transmission and diffraction and when the reference light or other special light wave used in the original record irradiates the hologram, the reconstructed light wave of the hologram decays, and the diffracted light wave is carried on the carrier, so the simulated image can be seen in this study. In order to confirm the above theory and principle in detail, the following detailed experiments are carried out in this study.

Suppose that in the plane, the sign of recording medium is h , so we can get the complex amplitude distribution formula of object light wave on it:

$$O(x, y) = o_o(x, y)\exp(-j\phi_o(x, y)). \quad (1)$$

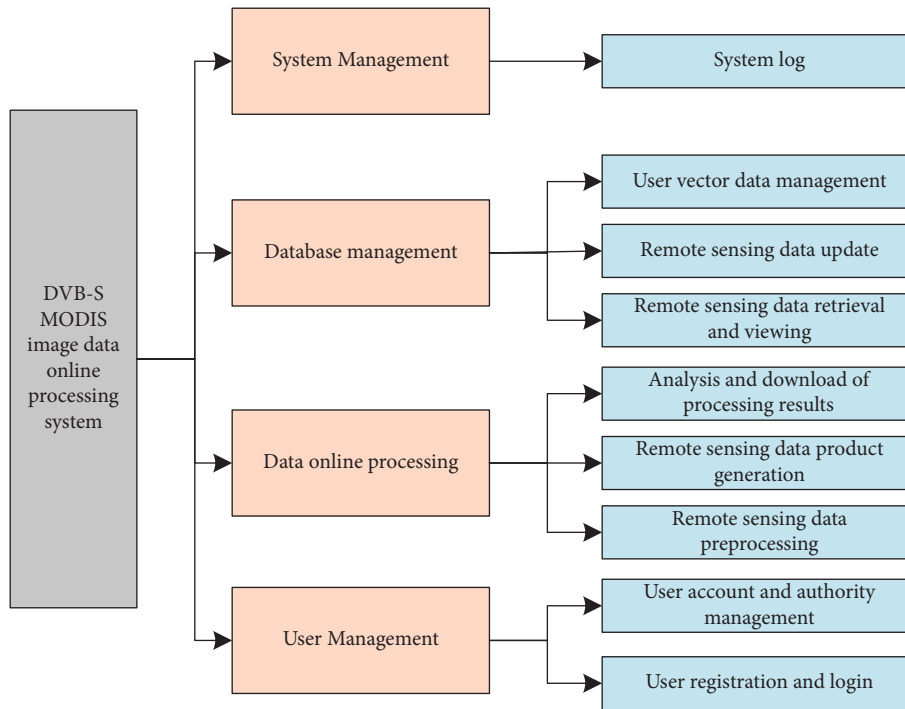


FIGURE 2: System function design.

TABLE 1: Content of system attribute data table.

Field name	Data type	Description
Img name	String	File name
Img path	String	File storage path
Img level	Integer	File level
Img classify	Integer	Data classification
Img type	String	File type/data source
Img time	String	Imaging time
Img dims	Integer	File dimension
Img reso	Float	Image spatial resolution
Img ext	Float	Image coverage
Cloud	Float	Cloud cover

TABLE 2: Image classification table.

Level	Types	Description
Level 0	Signal data	Raw sensor data received
IA level	DN value	Uncalibrated image data
IB level	DN value	Targeted data with geographic information
Level 2	Data product	Strip data inversion products
2G level	Data product	Projected and gridded inversion products

TABLE 3: Image data classification table.

Field name	Data type	Description
Img classify	Integer	Data classification number
Class name	String	Category name
Class name	String	Category information

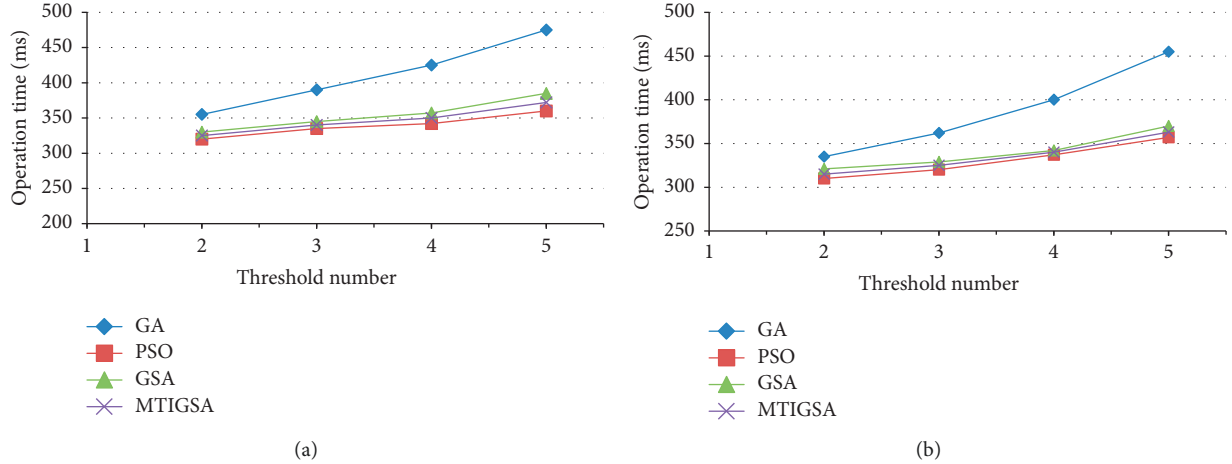


FIGURE 3: Computation time. (a) Butterfly (481*321). (b) Starfish (481*321).

The relevant reference light is added, and the plane wave for the reference light is selected:

$$R(x, y) = r_o(x, y)\exp(-j\varphi_x(x, y)). \quad (2)$$

Among them, $O_o(x, y)$ represents the amplitude distribution of the light of the object, $r_o(x, y)$ represents the amplitude distribution of the reference light, $\varphi_o(x, y)$ represents the phase division of the light of the object, and $\varphi_o(x, y)$ represents the phase distribution of the reference light. Then, the total light field on H can be expressed as follows:

$$U(x, y) = O(x, y) + R(x, y). \quad (3)$$

In the well-known optical holography, the optical film is always used to record the medium. After a series of related processing, the pattern is exposed. Through the developing process, the hologram is obtained in this paper. Through the above formula, we can know the intensity distribution of the object light and the reference light; due to the amplitude of the object light and the reference light, the phases of the object light and the reference light are mutually constrained; therefore, an interference term is set in this paper. The amplitude and phase information of the light of the object will include the amplitude and position information of the interference fringe.

Assume that it is within the curve area of linear t and within the function β'' . The resolution of the film used to record the hologram in this article will be very clear. Considering whether the intensity of the reference light is evenly distributed on the plane, according to the assumption, the following formula can be obtained:

$$t(x, y) = t_b + \beta|O|^2 + \beta'OR^* + \beta'O^*R. \quad (4)$$

Based on the above experimental results, only when the distances between the lines on the hologram are relatively close, the light waves can be significantly diffracted. When the original reference beam is irradiated on the hologram, a part of the original reference beam will be

diffracted by the hologram. When the hologram is far away from the reference beam, it will propagate in other directions. Just like the same light emitted by the original object, you can see the same three-dimensional image as the original object, so you can treat it as a virtual image of the object in its original position. If the reference beam used can meet the relevant reflection conditions, the direction of the obtained beam is opposite to the original beam. When the conjugate beam is irradiated from the back of the hologram, a real image will be generated and used as the original position of the object. Because light can directly produce the distribution image that this article wants, this real image can be detected directly without a lens or other photosensitive elements. Therefore, it can be concluded that the hologram plays a dual role of recording and projection.

Assuming that the complex amplitude distribution of the coherent light on the hologram surface is $C(x, y)$, then the distribution formula of the wave function is as follows:

$$U_t(x, y) = Ct_b + \beta'C|O|^2 + \beta'COR^* + \beta'CO^*R = U_1 + U_2 + U_3 + U_4. \quad (5)$$

If this article uses the original reference wave to illuminate and record the hologram, then $C(x, y) = R(x, y)$, the $U_1 = Ct_b = Rt_b$ in formula (5) is, whether the new light wave obtained in this paper is a plane wave or a spherical wave, its light wave amplitude will be changed separately; $U_2 = \beta''R|O|^2$ expresses the square term containing the complex amplitude characterizing the light wave properties of the object; in the $U_3 = \beta''|R|^2O(x, y)$ formula, $|R|^2$ represents the light intensity of the reference light, and its value is always a constant term. In addition, the reconstructed light wave of the original wavefront of the object light can be obtained; O^* in $U_4 = \beta''R^2O^*(x, y)$ formula represents the conjugate of the wavefront of the object light. Assuming that the conjugate light of the reference light is used to illuminate the hologram, that is, $C(x, y) = R^*(x, y)$, then U_3 and U_4 can also be expressed as follows:

$$U_3 = \beta' R^* R^* O, \quad (6)$$

$$U_4 = \beta' |R|^2 O^*. \quad (7)$$

Assuming that the medium used to propagate light is uniform and isotropic, then a specific scalar wave function can be used to set the light, where the light propagates along r , and the following formula can be obtained as follows:

$$E = E_0 \cos 2\pi \left(\frac{r}{\lambda} - \frac{t}{T} \right). \quad (8)$$

The above equation can be rewritten in the following equivalent form:

$$E = E_0 \cos(kr - \omega t). \quad (9)$$

Corresponding to the corresponding point, the above formula can be written as follows:

$$E(p, t) = E_0(p) \cos(2\pi vt - \phi(p)). \quad (10)$$

Point p light vibration state $E(p, t)$, period T , spatial frequency $\sigma = 1/\lambda$, and the phase of point P can be expressed in the following equivalent forms: $2\pi(r/\lambda - t/T)$, $(kr - \omega t)$, $(2\pi vt - \phi(p))$. The above formula represents the formula for the light vibration at any point p in a monochromatic plane wave field at time t . Among them, $E_0(p)$ represents the amplitude of vibration in the above formula, and $\phi(p)$ represents its initial phase. According to the relevant Euler's formula, the light vibration can be represented by a complex exponential function; that is, the $\phi(p)$ part of the phase related to the spatial position is separated from the $2\pi vt$ related to the time. Equation (10) can be rewritten in plural form as follows:

$$E(p, t) = \text{Re}\{E_0(p) \exp(-j[2\pi vt - \phi(p)])\} = \text{Re}\{E_0(p) e^{j\phi(p)} e^{-j2\pi vt}\}. \quad (11)$$

It is also possible to distribute the phase in the spatial frequency of the three coordinate axis directions:

$$\xi = \frac{1}{2\pi} \frac{\partial \phi}{\partial x} = \frac{\cos \alpha}{\lambda}, \eta = \frac{1}{2\pi} \frac{\partial \phi}{\partial y} = \frac{\cos \beta}{\lambda}, \zeta = \frac{1}{2\pi} \frac{\partial \phi}{\partial z} = \frac{\cos \gamma}{\lambda}. \quad (12)$$

The unit of dimension is circle/mm. When the angle between the propagation direction of light and the coordinate axis is an acute angle, the spatial frequency is positive; when the angle between the propagation direction of light and the coordinate axis is an obtuse angle, the spatial frequency is negative value, which is as follows:

$$U(x, y, z) = E_0(p) \exp[j2\pi(\xi x + \eta y + \zeta z)]. \quad (13)$$

Because of $\cos \beta = 0$,

$$U(x, y) = E \exp(jkx \cos \alpha). \quad (14)$$

If the obtained angle between the light propagation direction and the z -axis is set to θ , then

$$U(x, y) = E \exp(jkx \sin \theta). \quad (15)$$

The simplest and most basic form of wave surface is a spherical wave. For a monochromatic, divergent spherical wave, the complex amplitude of any point p in the light field can be expressed as follows:

$$U(p) = \frac{E_0}{r} e^{jkr}. \quad (16)$$

Among them, the wave number $k = 2\pi/\lambda$ means the phase change of the light wave per unit length; r is the point to be observed in this article; $p(x, y, z)$ is the distance from the light source; E_0 is the amplitude. Assuming that the spherical wave is convergent, then

$$U(p) = \frac{E_0}{r} e^{-jkr}. \quad (17)$$

If its origin is a point light source, or the origin is the point where light waves converge, then the propagation distance side can be expressed as follows:

$$r = (x^2 + y^2 + z^2)^{1/2}. \quad (18)$$

When the coordinate of the point light source is $s(x_0, y_0, z_0)$, and finally converge at a points (x_0, y_0, z_0) in space:

$$r = [(x - x_0)^2 + (y - y_0)^2 + (z - z_0)^2]^{1/2}. \quad (19)$$

We can study the complex amplitude distribution of the light field on a certain selected plane. As shown in the figure below, the point light source $s(x, y, 0)$ is located on the x_0, y_0 plane; after the propagation distance $z (z > 0)$, the light field distribution on the plane is as follows:

$$\begin{aligned} r &= [z^2 + (x - x_0)^2 + (y - y_0)^2]^{1/2} \\ &= z \left(1 + \frac{(x - x_0)^2 + (y - y_0)^2}{z^2} \right)^{1/2}. \end{aligned} \quad (20)$$

When only a small range of s angle is selected on the plane, the following formula is used:

$$\frac{(x - x_0)^2 + (y - y_0)^2}{z^2} \ll 1. \quad (21)$$

Putting the above equation into equation (13), we can get its complex amplitude on the xy plane as follows:

$$U(x, y) = \frac{E_0}{Z} \exp(jkz) \exp \left\{ j \frac{k}{2z} [(x - x_0)^2 + (y - y_0)^2] \right\}. \quad (22)$$

The formula after diffraction of light wave at point $H(x, y)$ is as follows:

$$U(x, y) = \frac{1}{j\lambda} \int_{\Sigma} O(x_0, y_0) \frac{e^{jkr}}{r} \cos \theta dx_0 dy_0. \quad (23)$$

Among them, $\cos \theta = d/r$, and when the propagation distance of the light wave is far or the selected area is small compared with the propagation distance, θ is smaller, which can be ignored:

$$U(x, y) = \frac{1}{j\lambda} \int_{\Sigma} O(x_0, y_0) \frac{e^{jkr}}{r} dx_0 dy_0. \quad (24)$$

The distance traveled by the light wave is calculated as follows:

$$r = \sqrt{d^2 + (x - x_0)^2 + (y - y_0)^2}. \quad (25)$$

According to the calculation result of the above formula, it can be concluded that the size of the reobtained image and the four physical quantities in the formula have a mutual relationship, and the distance is also one of the parameters that affect each quantity.

5. Conclusion

In today's Internet field, due to the continuous iterative update of computer simulation and interactive processing systems, the demand for computer simulation in all walks of life is increasing. In view of the complexity and professionalism of MODIS data preprocessing, DVB-SMODIS has developed interactive online processing functions for basic preprocessing. In order to allow nonprofessional remote sensing users to make better use of DVB-SMODIS data, using ASP.NET as the platform, the prototype system DVB-SMODIS for online interactive processing of remote sensing data has been developed. At the same time, in order to improve the efficiency of users' use of data, remote sensing image data and the improved BBO algorithm are also introduced. In order to compare the performance of the proposed algorithm, this paper compares it with other existing multithreshold image segmentation methods one by one. From the experimental conclusions, it can be shown that the algorithm proposed in this study is relative to other algorithms that have better segmentation results. The image segmentation method used at the beginning of this article only uses one-dimensional grayscale histogram in the selection of the threshold, and the important part of information such as the edge of the image is not referenced. Therefore, when the image is more complex, the obtained image is blurry. Therefore, in order to improve the substantive problems such as blurred images, this study proposes the algorithm based on the two-dimensional exponential cross-entropy multithreshold image segmentation, and the oblique division method replaces the direct division method, which is used to improve the problem of image blurring in the calculation of multithreshold image segmentation technology. The original multithreshold segmentation method is based on the search for the best segmentation threshold within the range of the existing evaluation function. Its wide search range makes the calculation very difficult. The intelligent optimization algorithm used today is very difficult to solve. In actual use, although it may not be able to obtain the best results, it can obtain a satisfactory solution in a relatively short time, which is more suitable for multithreshold selection problems. The objects actually photographed are encrypted and transmitted after computer simulation processing, so that objects in a larger area of the computer will be distorted as the angle

of the computer's recording increases. In order to make the recorded image more realistic and close to the original image, the distorted part should be restored. Therefore, this article is proposed to change the gray value of the image and restore the edge position of the image. The improved algorithm makes the computer simulation edge blur position close to the original image to a large extent.

Data Availability

The data used to support the findings of this study are available from the corresponding author upon request.

Conflicts of Interest

The authors declare that they have no conflicts of interest.

References

- [1] C. Hentschel, I. Blümel, and H. Sack, "Automatic annotation of scientific video material based on visual concept detection," *Proceedings of the 13th international conference on knowledge management and knowledge technologies, i-Know'*, vol. 13, no. 9, pp. 1–8, 2013.
- [2] U. S. Us, "Distance education IN architecture: emergency distance education IN architectural design studio and evaluation ON a sample," *Turkish Online Journal of Design Art and Communication*, vol. 11, no. 3, pp. 886–897, 2021.
- [3] H. Abdul-Kareem and S. Abdul-Kareem, "Retracted article: human-computer interaction using vision-based hand gesture recognition systems: a survey," *Neural Computing & Applications*, vol. 25, no. 2, pp. 251–261, 2014.
- [4] A. Maratea, A. Petrosino, and M. Manzo, "Generation of description metadata for video files," *Proceedings of the 14th inter-national conference on computer systems and technologies—CompSysTech'13*, vol. 76, no. 7, pp. 262–269, 2013.
- [5] F. Metzke, D. Ding, E. Younessian, and A. Hauptmann, "Beyond audio and video retrieval: topic-oriented multimedia summarization," *International Journal of Multimedia Information Retrieval*, vol. 2, no. 2, pp. 131–144, 2013.
- [6] P. Panchal, S. Merchant, and N. Patel, "Scene detection and retrieval of video using motion vector and occurrence rate of shot boundaries," *2012 Nirma University international conference on engineering (NUIcone)*, vol. 65, no. 9, pp. 1–6, 2012.
- [7] S. McCloskey and P. Davalos, "Activity detection in the wild using video metadata," *Pattern Recognition*, vol. 58, no. 7, pp. 3140–3143, 2012.
- [8] C. L. Wang and C. J. Wang, "A GA-based feature selection and parameters optimization for support vector machines," *Expert Systems with Applications*, vol. 31, no. 2, pp. 231–240, 2006.
- [9] D. S. Reddy and B. S. Reddy, "Digital image processing techniques for estimating power released from the corona discharges," *IEEE Transactions on Dielectrics and Electrical Insulation*, vol. 24, no. 1, pp. 75–82, 2017.
- [10] J. Matejka, T. Grossman, and G. Fitzmaurice, "Video lens: rapid playback and exploration of large video collections and associated metadata," in *Proceedings of the 27th annual ACM symposium on user interface software and technology, UIST'14*, vol. 82, no. 9, pp. 541–550, ACM, 2014.

- [11] S. S. Agrawal and A. Agrawal, "Vision based hand gesture recognition for human computer interaction: a survey," *Artificial Intelligence Review*, vol. 43, no. 1, pp. 1–54, 2015.
- [12] C.-C. Chang and C.-J. Lin, "LIBSVM: a library for support vector machines," *ACM Transactions on Intelligent Systems and Technology*, vol. 2, no. 3, 2011.
- [13] Z. Liu and H. Liu, "Human hand motion analysis with multisensory information," *IEEE*, vol. 19, no. 2, pp. 456–466, 2014.
- [14] C.-L. Dun and J.-F. Dun, "A distributed PSO-SVM hybrid system with feature selection and parameter optimization," *Applied Soft Computing*, vol. 8, no. 4, pp. 1381–1391, 2008.